

Low-Frequency Limit of Unified Models for Backscattering From Oceanlike Surfaces

Christophe Bourlier, *Member, IEEE*, and Nicolas Pinel, *Member, IEEE*

Abstract—In the context of electromagnetic-wave backscattering from oceanlike surfaces, by using the first two orders of unified models, like the small slope approximation and the local curvature approximation, we recently proposed an original technique to reduce the number of numerical integrations to two for easier numerical implementation. In this letter, this technique is simplified in the low-frequency limit, allowing us to bring a correction to the first-order small perturbation method.

Index Terms—Radar cross sections, remote sensing, sea surface electromagnetic scattering.

I. INTRODUCTION

FROM the 1960s, the derivation of the microwave backscattering normalized radar cross section (BNRCS) from oceanlike surfaces is a topic of investigation which is making progress and remains a challenging task. The first developed model is the Two-Scale Model [1], [2]. In the last two decades, another group of scattering models was proposed, namely, the *local unified* models [3]. One of the most popular is the small slope approximation (SSA) [4]; more recently, models based on the same decomposition of the scattering matrix as SSA were developed, like the local curvature approximation (LCA) [5], [6].

It is well known that such backscattering models are extremely difficult to implement in the full 3-D case, because of the fourfold integral that is involved (with two space variables and two frequency variables) and because of the strongly oscillating behavior of the integrand. That is why, recently, Bourlier and Pinel presented an original technique to reduce this computation to a twofold integral (with one space variable and one frequency variable) by resorting to the azimuthal harmonic expansion of the BNRCS and by using Bessel functions [7].

In this letter, this technique is tested in the low-frequency (LF) limit, allowing us to bring a correction to the first-order small perturbation method. This approximation allows us to significantly simplify the numerical implementation and to reduce the computing time of the BNRCS. In Section II, the technique developed by Bourlier and Pinel is briefly summarized, and in Section III, it is simplified in the LF limit. In Section IV, numerical comparisons are presented.

Manuscript received October 22, 2009; revised December 3, 2009. Date of publication February 22, 2010; date of current version April 29, 2010.

The authors are with the Institut de Recherche en Electrotechnique et Electronique de Nantes Atlantique (IREENA) Laboratory, Université Nantes Angers Le Mans, Polytech'Nantes, 44306 Nantes Cedex 3, France (e-mail: christophe.bourlier@polytech.univ-nantes.fr).

Color versions of one or more of the figures in this paper are available online at <http://ieeexplore.ieee.org>.

Digital Object Identifier 10.1109/LGRS.2010.2040366

II. BNRCS OF UNIFIED MODELS

In the literature, from microwave experimental data (for instance, see [9] and the references therein), it was established that the BNRCS can be expressed for $pq = \{VV, HH\}$ copolarizations in the form

$$\sigma^{pq}(\theta, \phi; u) = \sigma_0^{pq}(\theta; u) + \sigma_2^{pq}(\theta; u) \cos(2\phi) \quad (1)$$

where ϕ is the observation azimuthal angle with respect to the wind direction, θ is the observation elevation angle, and u is the wind speed. In addition, $\sigma_1^{pq}(\theta; u) = 0$ (coefficient along $\cos \phi$) because the surface is assumed to be Gaussian. By considering the first two orders of the kernels of unified models, $\hat{\mathcal{N}}^{pq}(\theta, \phi; \xi) \approx \mathcal{N}_1^{pq}(\theta, \phi) + \hat{\mathcal{N}}_2^{pq}(\theta, \phi; \xi)$, which depend on the chosen model, the BNRCS is equal to the sum of two terms, $\sigma^{pq}(\theta, \phi; u) = \sigma_{11}^{pq}(\theta, \phi; u) + \sigma_{12}^{pq}(\theta, \phi; u)$. The subscript “11” results from the autocorrelation of the first-order scattered field, whereas the subscript “12” results from the cross correlation between the first- and second-order scattered fields.

Bourlier and Pinel recently showed that the BNRCS even harmonics $\{\sigma_{11,0}^{pq}(\theta; u), \sigma_{11,2}^{pq}(\theta; u)\}$ related to “11” can be expressed as [7]

$$\begin{cases} \sigma_{11,0}^{pq}(\theta; u) = A_1 \int_0^\infty J_0(a)[e^{\beta} I_0(b) - 1]rdr \\ \sigma_{11,2}^{pq}(\theta; u) = 2A_1 \int_0^\infty e^{\beta} J_2(a)I_1(b)rdr \end{cases} \quad (2)$$

where

$$\begin{cases} a(r) = 2Kr \sin \theta, & b(r) = Q_z^2 W_2(r) \\ \beta(r) = Q_z^2 W_0(r), & A_1 = 2\pi A |\mathcal{N}_1^{pq}(\theta)|^2 e^{-Q_z^2 \sigma_\eta^2} \\ A = \frac{1}{\pi Q_z^2}, & Q_z = 2K \cos \theta. \end{cases} \quad (3)$$

In addition

$$\begin{cases} W_2(r, \phi_r) = W_0(r) - \cos(2\phi_r)W_2(r) \\ W_0(r) = \int_0^\infty \hat{W}_0(\xi)J_0(r\xi)d\xi \\ W_2(r) = \int_0^\infty \hat{W}_2(\xi)J_2(r\xi)d\xi \end{cases} \quad (4)$$

where \hat{W}_0 and \hat{W}_2 stand for the isotropic and anisotropic parts of the sea spectrum, respectively. W_0 and W_2 are their respective associated correlation functions, and $\sigma_\eta^2 = W_0(0)$ is the height variance. In polar coordinates (ξ, ϕ_ξ) , the sea spectrum is assumed to be

$$\hat{W}(\xi, \phi_\xi) = [\hat{W}_0(\xi) + \hat{W}_0(\xi) \cos(2\phi_\xi)]/(2\pi) \quad (5)$$

which is consistent with the sea spectrum of Elfouhaily *et al.* [8]. J_m and I_m are the Bessel functions of the first and second kinds, respectively, and of order m . Equation (2) shows that the BNRCS is obtained from a single numerical integration over the radial distance r .

For the LCA2 model, we have ($\nu = 0$)

$$\begin{aligned} \sigma_{12,n}^{\text{pq}}(\theta; u) &= 2A\pi e^{-Q_z^2\sigma_\eta^2} \int_0^\infty \int_0^\infty r d\xi dr \hat{G}_0^{\text{pq}}(\xi) \\ &\times \left(\hat{W}_0(\xi) J_n(a) \{ e^\beta I_{\frac{n}{2}}(b) [J_0(c) - 1] + \delta_{n,0} \} \right. \\ &+ \frac{1}{2} \hat{W}_2(\xi) e^\beta J_n(a) J_2(c) \\ &\left. \times \left[I_{\frac{n-2}{2}}(b) + I_{\frac{n+2}{2}}(b) \right] \right), \quad n \text{ is even} \end{aligned} \quad (6)$$

where

$$\hat{G}_s^{\text{pq}}(\xi) = \frac{1}{2\pi} \int_0^{2\pi} \hat{G}^{\text{pq}}(\xi, \phi_\xi - \nu\phi) e^{-js(\phi_\xi - \nu\phi)} d(\phi_\xi - \nu\phi) \quad (7)$$

$$\begin{cases} \hat{G}^{\text{pq}}(\xi, \phi_\xi) = -2Q_z \text{Im} \left[(\mathcal{N}_1^{\text{pq}})^* \hat{\mathcal{N}}_2^{\text{pq}}(\xi, \phi_\xi) \right] \\ \hat{G}^{\text{pq}}(\xi, \phi_\xi) = -2Q_z \text{Im} \left[(\mathcal{N}_1^{\text{pq}})^* \hat{\mathcal{N}}_2^{\text{pq}}(\xi, \phi_\xi) \right] \\ \quad + \left| \hat{\mathcal{N}}_2^{\text{pq}}(\xi, \phi_\xi) \right|^2 \quad \text{PPT} \end{cases} \quad (8)$$

$c = \xi r$, and $\delta_{n,m}$ is the Kronecker symbol such that $\delta_{n,m} = 1$ if $n = m$ and zero if otherwise. Equation (7) is the Fourier series of the kernel $\hat{G}^{\text{pq}}(\xi, \phi_\xi)$ expressed from the first $\mathcal{N}_1^{\text{pq}}(\theta, \phi)$ - and second $\mathcal{N}_2^{\text{pq}}(\theta, \phi; \xi, \phi_\xi)$ -order kernels. In the backscattering direction, their expression can be found in [7]. To simplify the derivation of the BNRCS, the phase perturbation technique (PPT) is often applied, which implies a new definition of the kernel $\hat{G}^{\text{pq}}(\xi, \phi_\xi)$. For more details, see [7].

For the SSA2 model, we have ($\nu = 1$)

$$\begin{aligned} \sigma_{12,n}^{\text{pq}}(\theta; u) &= 2A\pi e^{-Q_z^2\sigma_\eta^2} \int_0^\infty \int_0^\infty r d\xi dr \\ &\times \left(\hat{W}_0(\xi) \left\{ e^\beta \left[\Omega_n^{(0)}(a, b, c) - \hat{G}_0^{\text{pq}}(\xi) I_{\frac{n}{2}}(b) J_n(a) \right] \right. \right. \\ &+ \hat{G}_0^{\text{pq}}(\xi) J_0(a) \delta_{n,0} \Big\} \\ &+ \hat{W}_2(\xi) \left\{ e^\beta \left[\Omega_n^{(2)}(a, b, c) - \hat{G}_2^{\text{pq}}(\xi) \right. \right. \\ &\times \sum_{\gamma=\pm 1} J_{n\gamma+2}(a) I_{\frac{n\gamma+2}{2}}(b) \Big] \\ &\left. \left. + \hat{G}_2^{\text{pq}}(\xi) J_0(a) \delta_{n,\pm 2} \right\} \right), \quad n \text{ is even} \end{aligned} \quad (9)$$

with $\hat{G}_{-s} = \hat{G}_s \in \mathbb{R}$. The functions $\Omega_n^{(0)}(a, b, c)$ and $\Omega_n^{(2)}(a, b, c)$ are expressed from sums of Bessel functions. They are given by equations (42) and (43) in [7], respectively. Unlike the LCA2 model, the SSA2 model requires the computation of a sum over s . For $s = 0$, corresponding to the LCA2 model, (6) is found.

The SSA2 requires the computation of a sum because its second-order subkernel $\mathcal{N}_2^{\text{pq}}(\theta, \phi; \xi, \phi_\xi)$ depends on the angle

$\phi - \phi_\xi$, whereas the LCA2 second-order subkernel is isotropic, since it is independent of $\phi - \phi_\xi$. This fundamental difference implies that the derivations led for the SSA2 model are more complicated than that for the LCA2 model. It is also important to note that (9) is valid for any kernel $\mathcal{N}_2^{\text{pq}}(\theta, \phi; \xi, \phi_\xi)$ obeying the same properties as SSA2 or LCA2.

The next section simplifies the equations by applying the LF limit. For the SSA2 model, it is equivalent to extending the SPM-1 by adding the contribution related to the subkernel $\mathcal{N}_2^{\text{pq}}(\theta, \phi; \xi, \phi_\xi)$. Typically, for an oceanlike surface, the SPM-1 can be applied for $\theta \gtrsim 30^\circ$. The higher order of the LCA-1 model is not a correction to the SPM-1, because its first order satisfies the first-order Kirchoff (KA-1) approximation.

III. BNRCS IN THE LF LIMIT

Under the SPM-1, the Rayleigh roughness parameter $Q_z \sigma_\eta = 2K\sigma_\eta \cos \theta$ is assumed to be much smaller than one. Then, the integrands of (2) can be expanded as

$$\begin{cases} e^\beta I_0(b) - 1 = \beta + \mathcal{O}(Q_z^3) \\ e^\beta I_1(b) = b/2 + \mathcal{O}(Q_z^3). \end{cases} \quad (10)$$

Substituting (10) into (2) and using (4) and (11) [13]

$$\forall s \in \mathbb{Z}, \quad \int_0^\infty r J_s(\xi r) J_s(k_B r) dr = \delta(\xi - k_B)/\xi \quad (11)$$

we obtain

$$\begin{cases} \sigma_{11,0}^{\text{pq}}(\theta; u) = 2 |\mathcal{N}_1^{\text{pq}}(\theta)|^2 \hat{W}_0(k_B)/k_B \\ \sigma_{11,2}^{\text{pq}}(\theta; u) = \sigma_{11,0}^{\text{pq}}(\theta; u) \hat{\Delta}(k_B). \end{cases} \quad (12)$$

As expected, under the SPM-1 limit, the BNRCS is proportional to the sea spectrum evaluated at the Bragg wavenumber $\xi = k_B$.

For the case $\hat{\mathcal{N}}_2^{\text{pq}}(\xi) \neq 0$, first, a series expansion over Q_z up to the first order is considered. Thus

$$e^\beta I_n(b) = \delta_{n,0} + \mathcal{O}(Q_z^2). \quad (13)$$

The functions $\Omega_n^{(0)}(a, b, c)$ and $\Omega_n^{(2)}(a, b, c)$ [7, eqs. (42) and (43)] can be simplified from their substitutions into (9) and by using (11). Then, the integrations over r and ξ lead the SSA2 model to

$$\begin{cases} \sigma_{12,0}^{\text{pq}}(\theta; u) = \frac{\hat{W}_0(k_B)}{2k_B K^2 \cos^2 \theta} \sum_{s=-\infty}^{+\infty} (-1)^s \hat{G}_s(k_B) \\ \sigma_{12,2}^{\text{pq}}(\theta; u) = \frac{\sigma_{12,0}^{\text{pq}}(\theta; u) \hat{\Delta}(k_B)}{2}. \end{cases} \quad (14)$$

The sum over s can be reduced to $s \in \mathbb{N}$, since $\hat{G}_{-s} = \hat{G}_s \in \mathbb{R}$. The BNRCS is then very simple and is equal to the sum of the Fourier series coefficients, which depend on the first- and second-order subkernels.

For the LCA2 model, since $\hat{G}_{|s|} = 0$ for $|s| > 0$, we have

$$\sigma_{12,0}^{\text{pq}}(\theta; u) = \frac{\hat{W}_0(k_B) \hat{G}_0(k_B)}{2k_B K^2 \cos^2 \theta} \quad \sigma_{12,2}^{\text{pq}} = \frac{\sigma_{12,0}^{\text{pq}} \hat{\Delta}(k_B)}{2}. \quad (15)$$

Thus, the use of the LF limit makes it possible to remove the twofold numerical integrations [see (6)] over r and ξ .

In addition, like for the SPM-1 model, the BNRCS is related to the sea spectrum computed at $\xi = k_B$ but multiplied by the kernel $\hat{G}_0(k_B)$. For a perfectly conducting surface, the expressions of the LCA2 subkernels are very simple. See for instance [7, Appendix D]. Then, we have

$$\hat{\mathcal{N}}_2^{\text{VV},\text{HH}} = -\frac{jQ_z\xi^2}{2} \quad \hat{\mathcal{N}}_1^{\text{VV}} = 2K^2 \quad \hat{\mathcal{N}}_1^{\text{HH}} = -2K^2 \quad (16)$$

leading from (8) to

$$\begin{cases} \sigma_{12,0}^{\text{pq}}(\theta; u) = \pm 8\hat{W}_0(k_B)K^3 \sin \theta \\ \sigma_{12,0}^{\text{pq}}(\theta; u) = 8\hat{W}_0(k_B)K^3 \sin \theta (\pm 1 + \sin^2 \theta / 2). \end{cases} \quad (17)$$

The sign + corresponds to the VV polarization, whereas the sign - corresponds to the HH polarization. For a highly conducting surface ($|\epsilon_r| \gg 1$), like the sea surface, we have

$$\begin{cases} \sigma_{12,0}^{\text{pq}}(\theta; u) \approx \frac{4}{K} |\hat{\mathcal{N}}_1^{\text{pq}}(\theta)|^2 \hat{W}_0(k_B) \sin \theta \times \text{Re}(\alpha^{\text{pq}}) \\ \sigma_{12,0}^{\text{pq}}(\theta; u) \approx \frac{4}{K} |\hat{\mathcal{N}}_1^{\text{pq}}(\theta)|^2 \hat{W}_0(k_B) \sin \theta \\ \quad \times [\text{Re}(\alpha^{\text{pq}}) + \sin^2 \theta |\alpha^{\text{pq}}|^2] \end{cases} \quad (18)$$

where $\alpha^{\text{VV}} = -1/2$ and $\alpha^{\text{HH}} = 1/2 + \tan^2 \theta / \epsilon_r$. The next section shows that a series expansion over Q_z up to the first order is enough for the LCA2 model, unlike for the SSA2 model. Indeed, by substituting (7) into (14), the sum over s , i.e., $\sum_s (-1)^s \hat{G}_s(k_B)$, vanishes since $\sum_s (-1)^s e^{-js\alpha} = 0$. Thus, a series expansion up to the second order is needed, leading to more complex derivations, which are reported in the Appendix. It is then shown for the SSA2 model that

$$\begin{cases} \frac{\sigma_{12,0}^{\text{pq}}(\theta; u)}{2} = \Psi_{0,0}(0, 1) - \Lambda_{0,0}(0) + \frac{1}{2} [\Psi_{2,2}(k_B, \xi_w) - \Lambda_{2,2}(1)] \\ \frac{\sigma_{12,2}^{\text{pq}}(\theta; u)}{2} = \Psi_{2,0}(1, 1) - \Lambda_{2,0}(1) + \frac{1}{2} [\Psi_{0,2}(\xi, \xi_w) - \Lambda_{0,2}(0)] \end{cases} \quad (19)$$

where

$$\begin{cases} \Psi_{n,m}(u, v) = \frac{1}{2\pi} \int_0^{2\pi} \int_0^\infty \frac{\hat{W}_n(\xi) \hat{W}_m(\xi_w)}{\xi_w} \\ \quad \times \hat{G}^{\text{pq}}(\xi, -\alpha - \pi) \left(1 - \frac{2u \sin^2 \alpha}{v} \right) d\alpha d\xi \\ \Lambda_{n,m}(u) = \frac{\hat{W}_n(k_B)}{k_B} \frac{1}{2\pi} \int_0^{2\pi} \int_0^\infty \hat{W}_m(\xi) \hat{G}^{\text{pq}}(\xi, \alpha) \\ \quad \times (1 - 2u \sin^2 \alpha) d\alpha d\xi \\ \xi_w = \sqrt{\xi^2 + k_B^2 - 2\xi k_B \cos \alpha}. \end{cases} \quad (20)$$

The aforementioned equations show that $\sigma_{12,0}^{\text{pq}}(\theta; u)$ is expressed from a double integral, in which the product of two spectra, computed at ξ and $\xi_w \in [|\xi - k_B|; \xi + k_B]$ (as functions of ξ and k_B), occurs. This behavior can be interpreted as a convolution product expressed in polar coordinates, which is characteristic of the SPM-2 limit, satisfied by the SSA2 model. Like for (9), the BNRCS requires the computation of twofold numerical integrations over the radial distance r and the angle α . However, the BNRCS does not require the calculation of the Fourier series coefficients $\{\hat{G}_s^{\text{pq}}(\xi)\}$ [see (7)] and of the sum over s . Thus, the numerical implementation of (19) is much easier than that of (9).

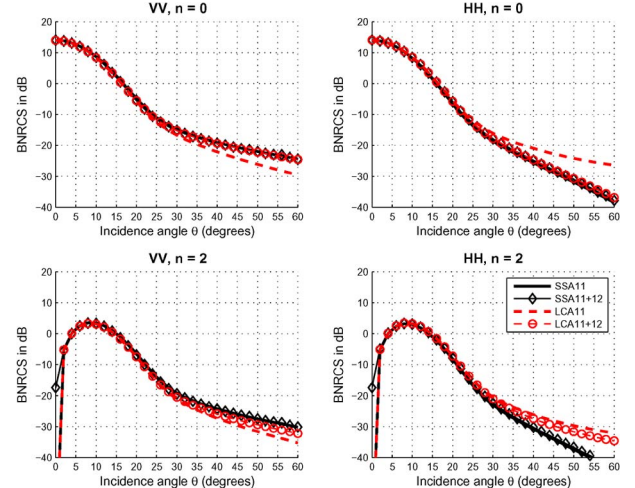


Fig. 1. BNRCS computed from the SSA2 and LCA2 models versus the incidence angle θ for $f = 14$ GHz and $u_{10} = 5$ m/s. At the top, $n = 0$ (zero-order harmonic), and at the bottom, $n = 2$ (second-order harmonic). On the left is VV polarization, and on the right is HH polarization.

IV. NUMERICAL RESULTS

The numerical evaluations of the BNRCSs $\{\sigma_{11,0}^{\text{pq}}, \sigma_{11,2}^{\text{pq}}\}$ given by (2), (6), and (9) are explained in detail in [7]. With the use of the LF limit, the LCA2 numerical implementation [see (15), (17), and (18)] is very easy, because no numerical integration is needed. In addition, for a given incidence angle θ , on a PC with 4 GB of RAM and a processor of 3 GHz, the computing time for the SSA2 is on the order of 0.1 s.

The aim of this letter is not to compare the different backscattering models with measurements. This was already done thoroughly in previous works [10]–[12] (see also references therein). The scope of this letter is to study the accuracy of the LF limit. As shown by Bourlier and Pinel [7], the LCA2 model gives nonphysical results for the HH polarization when the PPT is not applied, whereas the SSA2 model gives the same results with and without the use of the PPT. Thus, in the following, only the PPT is tested.

Fig. 1 shows the BNRCS computed from the SSA2 and LCA2 models versus the incidence angle θ for $f = 14$ GHz and $u_{10} = 5$ m/s. As can be seen, the LCA2 second-order contribution “12” is larger than the SSA2 one and is positive for the HH polarization, whereas it is negative for the VV polarization. It can be noted that the LCA11 satisfies the KA-1 limit, whereas the SSA11 satisfies the SPM-1 limit, which explains their different behaviors for $\theta \gtrsim 25^\circ$.

Fig. 2 shows the harmonics ($n = 0$ and $n = 2$) of the ratio $|\sigma_n^{\text{pq},\text{LF}}/\sigma_n^{\text{pq}}|$ computed from the SSA2 model versus the incidence angle $\theta \in [0; 60]$ in degrees for $f = 14$ GHz (Ku-band, sea relative permittivity $\epsilon_r = 47 + j38$), $u_{10} = 5$ m/s, and VV and HH polarizations. Fig. 3 shows the same parameters as in Fig. 2, but for the LCA2 model. In the legends of Figs. 2 and 3, the label “11-LF+12-LF” means that the LF is applied to both 11 and 12, and the label “11+12-LF” means that the LF is applied only to 12. For the LCA2 model, the label “11+12-LF-HC” means that (18) is used for the computation of σ_{12} , whereas σ_{11} is computed without approximation.

For θ close to zero, Figs. 2 and 3 clearly show that the LF approximation cannot be applied to the 11 order (SPM-1). For the SSA2 model, as θ increases, the ratio computed from the use of the LF approximation tends toward the one without

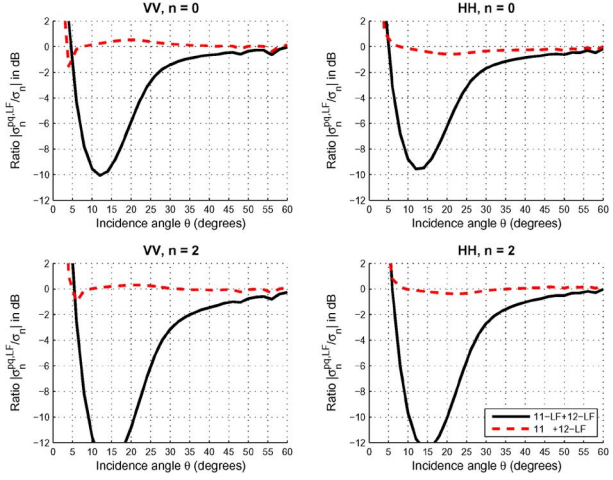


Fig. 2. Ratio $|\sigma_n^{pq,LF}/\sigma_n^{pq}|$, in decibel scale, computed from the SSA2 model versus the incidence angle θ for $f = 14$ GHz and $u_{10} = 5$ m/s.

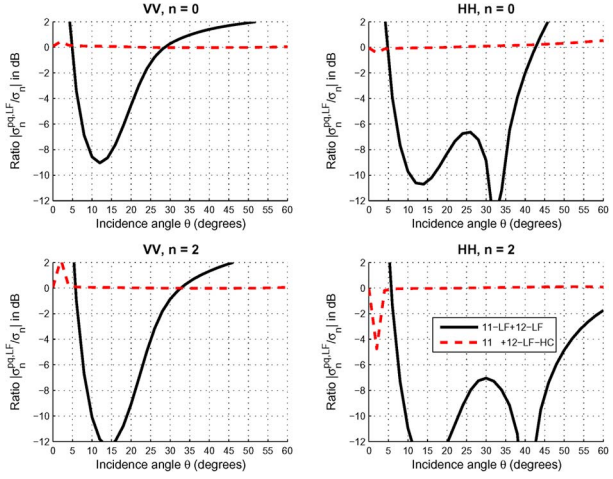


Fig. 3. Same as in Fig. 2, but for the LCA2 model.

TABLE I

MEAN VALUE OF THE DIFFERENCE IN DECIBEL SCALE FOR THE SSA2 AND LCA2 MODELS, RESPECTIVELY. u_{10} IS IN METERS PER SECOND AND f IS IN GIGAHERTZ

u_{10}, f	VV, $n = 0$	HH, $n = 0$	VV, $n = 2$	HH, $n = 2$
5, 5.3	0.167	-0.253	0.046	-0.004
10, 5.3	0.166	-0.298	0.047	-0.032
5, 14	0.171	-0.308	0.047	-0.044
10, 14	0.204	-0.374	0.056	-0.062
5, 5.3	0.000	0.154	0.002	0.052
10, 5.3	0.140	0.034	0.118	-0.029
5, 14	0.006	0.176	0.012	0.049
10, 14	0.104	0.125	0.010	-0.019

approximation. For the LCA2 model, Fig. 3 shows, for any θ , that the results computed from the LF approximation match very well the results with no approximation. For small θ , Fig. 3 shows a difference between the results, but has no impact on the total BNRCS (not depicted here). This result is very interesting because the use of the LF approximation leads to a very simple model of the BNRCS, which is very easy to implement numerically.

Table I gives the values of $\delta = \text{mean}_{\theta \in [10;60]^\circ} |\sigma_n^{pq,LF}/\sigma_n^{pq}|$ (in decibels, red dashed-line curves in Figs. 2 and 3) for different frequencies f (in gigahertz) and wind speeds u_{10} (in meters per second). As can be seen, δ is not much sensitive to the wind speed and the frequency.

V. CONCLUSION

In this letter, under the LF limit, the numerical implementation of the sea BNRCS has been simplified for local unified models and tested on the LCA2 and SSA2 kernels. For the SSA2 model, the BNRCS computation requires the evaluation of a 2-D integral over the wavenumber ξ and the angle α , which strongly reduces the numerical complexity, comparatively with the case for which no assumption is used (4-D integral). For the LCA2 model, a very simple closed-form expression of the BNRCS, which requires no numerical integration, is obtained. It is then shown that the BNRCS is proportional to the sea spectrum multiplied by the LCA kernel and evaluated at the Bragg frequency.

Simulations led for microwave frequencies show that the SSA2 model with the LF limit tends toward the SSA2 model with no approximation when the incidence angle increases. For the LCA2 model, the agreement is even better as the results with and without approximations do not highlight significant differences for all incidence angles. Thus, the LF limit is very useful for moderate incidence angles (smaller than 80° – 85°) because the numerical integrations over $\{r, \xi\}$ in (6) and (9) become very difficult, since the integrand strongly oscillates and slowly decreases. Like in [7], let us recall that the derivations led in this letter are general and can be used for other kinds of scattering kernels.

APPENDIX

Using a series expansion over Q_z up to the second order, from [7, eq. (42)], the term $e^{\beta}\Omega_n^{(0)}(a, b, c)$ in (9) becomes

$$\left\{ \begin{array}{l} e^{\beta}\Omega_0^{(0)}(a, b, c) = \Omega_0^{(0)}(a, 0, c) + \beta \\ \quad \times \sum_{s=-\infty}^{+\infty} (-1)^s \hat{G}_s^{pq}(\xi) J_s(c) J_s(a) + \mathcal{O}(Q_z^3) \\ e^{\beta}\Omega_2^{(0)}(a, b, c) = \Omega_2^{(0)}(a, 0, c) + b \\ \quad \times \sum_{s=-\infty}^{+\infty} \frac{(-1)^s}{4} \hat{G}_s^{pq}(\xi) J_s(c) \left[\sum_{\gamma=\pm 1} J_{2\gamma+s}(a) \right] \\ \quad + \mathcal{O}(Q_z^3) \end{array} \right. \quad (A1)$$

where

$$e^{\beta}I_0(b) = 1 + \beta \quad e^{\beta}I_1(b) = b/2 \quad e^{\beta}I_n(b) = 0 \quad (A2)$$

up to the order Q_z^2 , where $I_{-1}(b) = I_1(b)$ and $n > 1$. In the same way, from [7, eq. (43)], the term $e^{Q_z^2 W_0(r)}\Omega_n^{(2)}(a, b, c)$ in (9) becomes

$$\left\{ \begin{array}{l} e^{Q_z^2 W_0(r)}\Omega_0^{(2)}(a, b, c) = \Omega_0^{(2)}(a, 0, c) + Q_z^2 W_2(r) \\ \quad \times \sum_{s=-\infty}^{+\infty} \frac{(-1)^s}{4} \hat{G}_s^{pq}(\xi) J_s(a) \\ \quad \times \left[\sum_{\gamma=\pm 1} J_{s+2\gamma}(c) \right] + \mathcal{O}(Q_z^3) \\ e^{Q_z^2 W_0(r)}\Omega_2^{(2)}(a, b, c) = \Omega_2^{(2)}(a, 0, c) + Q_z^2 W_0(r) \\ \quad \times \sum_{s=-\infty}^{+\infty} \frac{(-1)^s}{2} \hat{G}_s^{pq}(\xi) \\ \quad \times \left[\sum_{\gamma=\pm 1} J_{2\gamma+s}(a) J_{2\gamma+s}(c) \right] \\ \quad + \mathcal{O}(Q_z^3). \end{array} \right. \quad (A3)$$

The use of the Graf addition theorem [13] on the Bessel functions leads to

$$J_p(w)e^{jpx} = \sum_{s=-\infty}^{+\infty} J_{p+s}(u)J_s(v)e^{js\alpha} \quad (\text{A4})$$

with

$$\begin{cases} w = \sqrt{u^2 + v^2 - 2uv \cos \alpha}, & v \sin \alpha = w \sin \chi \\ u - v \cos \alpha = w \cos \chi. \end{cases} \quad (\text{A5})$$

By the substitution of (A4) into (7) and (A1) and since $(-1)^s \hat{G}_s^{\text{pq}}(\xi) = \hat{G}_s^{\text{pq}}(\xi)e^{-s\pi}$, one obtains

$$\begin{aligned} Q_z^2 W_0(r) & \sum_{s=-\infty}^{+\infty} (-1)^s \hat{G}_s^{\text{pq}}(\xi) J_s(c) J_s(a) \\ &= \frac{Q_z^2 W_0(r)}{2\pi} \int_0^{2\pi} J_0(r\xi_w) \hat{G}^{\text{pq}}(\xi, \phi_\xi) d\alpha \end{aligned} \quad (\text{A6})$$

$$\begin{aligned} Q_z^2 W_2(r) & \sum_{s=-\infty}^{+\infty} \frac{(-1)^s \hat{G}_s^{\text{pq}}(\xi)}{4} J_s(c) \sum_{\gamma=\pm 1} J_{2\gamma+s}(a) \\ &= \frac{Q_z^2 W_2(r)}{4\pi} \int_0^{2\pi} \hat{G}^{\text{pq}}(\xi, \phi_\xi) J_2(r\xi_w) \cos(2\chi) d\alpha \end{aligned} \quad (\text{A7})$$

where

$$\xi_w = \frac{w}{r} = \sqrt{\xi^2 + k_B^2 - 2\xi k_B \cos \alpha}, \quad \alpha = \phi - \phi_\xi - \pi \quad (\text{A8})$$

in which ξ_w is independent of r .

In the same way, from (A3), one obtains

$$\begin{aligned} Q_z^2 W_2(r) & \sum_{s=-\infty}^{+\infty} \frac{(-1)^s \hat{G}_s^{\text{pq}}(\xi)}{4} J_s(a) \sum_{\gamma=\pm 1} J_{2\gamma+s}(c) \\ &= \frac{Q_z^2 W_2(r)}{4\pi} \int_0^{2\pi} \hat{G}^{\text{pq}}(\xi, \phi_\xi) J_2(r\xi_w) \cos(2\chi) d\alpha \end{aligned} \quad (\text{A9})$$

$$\begin{aligned} Q_z^2 W_0(r) & \sum_{s=-\infty}^{+\infty} \frac{(-1)^s \hat{G}_s^{\text{pq}}(\xi)}{2} \sum_{\gamma=\pm 1} J_{2\gamma+s}(a) J_{2\gamma+s}(c) \\ &= \frac{Q_z^2 W_0(r)}{2\pi} \int_0^{2\pi} \hat{G}^{\text{pq}}(\xi, \phi_\xi) J_0(r\xi_w) \cos(2\alpha) d\alpha. \end{aligned} \quad (\text{A10})$$

It can be noted that

$$\cos(2\chi) = \begin{cases} 1 - \frac{2\xi \sin^2 \alpha}{\xi_w}, & \text{in (A7) } (u = a, v = c) \\ 1 - \frac{2k_B \sin^2 \alpha}{\xi_w}, & \text{in (A9) } (u = c, v = a) \end{cases} \quad (\text{A11})$$

which is independent of the radial distance r .

The use of (4) and (11) yields

$$\begin{cases} \int_0^\infty W_0(r) J_0(r\xi_w) r dr \\ = \int_0^\infty \hat{W}_0(\xi') \times [\int_0^\infty J_0(r\xi') J_0(r\xi_w) r dr] d\xi' = \frac{\hat{W}_0(\xi_w)}{\xi_w} \\ \int_0^\infty W_2(r) J_2(r\xi_w) r dr \\ = \int_0^\infty \hat{W}_2(\xi') \times [\int_0^\infty J_2(r\xi') J_2(r\xi_w) r dr] d\xi' = \frac{\hat{W}_2(\xi_w)}{\xi_w} \end{cases} \quad (\text{A12})$$

Thus, the integration over r in (A6), (A7), (A9), and (A10) multiplied by r leads to

$$\begin{cases} \int_0^\infty [(\text{A6})] r dr = \frac{Q_z^2}{2\pi} \int_0^{2\pi} \frac{\hat{W}_0(\xi_w) \hat{G}^{\text{pq}}(\xi, -\alpha - \pi)}{\xi_w} d\alpha \\ \int_0^\infty [(\text{A7})] r dr = \frac{Q_z^2}{4\pi} \int_0^{2\pi} \frac{\hat{W}_2(\xi_w) \hat{G}^{\text{pq}}(\xi, -\alpha - \pi)}{\xi_w} \\ \times \left(1 - \frac{2\xi \sin^2 \alpha}{\xi_w}\right) d\alpha \\ \int_0^\infty [(\text{A9})] r dr = \frac{Q_z^2}{4\pi} \int_0^{2\pi} \frac{\hat{W}_2(\xi_w) \hat{G}^{\text{pq}}(\xi, -\alpha - \pi)}{\xi_w} \\ \times \left(1 - \frac{2k_B \sin^2 \alpha}{\xi_w}\right) d\alpha \\ \int_0^\infty [(\text{A10})] r dr = \frac{Q_z^2}{2\pi} \int_0^{2\pi} \frac{\hat{W}_0(\xi_w) \hat{G}^{\text{pq}}(\xi, -\alpha - \pi)}{\xi_w} \\ \times (1 - 2 \sin^2 \alpha) d\alpha \end{cases} \quad (\text{A13})$$

respectively. From (9), the derivation of $\sigma_{12,n}^{\text{pq}}(\theta; u)$ also requires the integrations of $\hat{G}_0^{\text{pq}}(\xi) I_{n/2}(b) J_n(a) = \Omega_n^{(0)}(a, b, 0)$ and $\sum_{\gamma=\pm 1} J_{n\gamma+2}(a) I_{n\gamma+2/2}(b) = \Omega_n^{(2)}(a, b, 0)$. Using the fact that $J_n(0) \neq 0$ for $n = 0$, from (A1), (A3), and (11), they are obtained from (A13) by taking $c = 0$.

ACKNOWLEDGMENT

The authors would like thank the anonymous reviewers for their useful comments and suggestions.

REFERENCES

- [1] B. F. Kur'yanov, "The scattering of sound at a rough surface with two types of irregularity," *Sov. Phys. Acoust.*, vol. 8, pp. 252–257, 1963.
- [2] J. W. Wright, "A new model for sea clutter," *IEEE Trans. Antennas Propag.*, vol. 16, no. 2, pp. 217–223, Mar. 1968.
- [3] T. M. Elfouhaily and C.-A. Guérin, "A critical survey of approximate scattering wave theories from random rough surfaces," *Waves Random Complex Media*, vol. 14, no. 4, pp. R1–R40, Oct. 2004.
- [4] A. G. Voronovich, *Wave Scattering From Rough Surfaces*, 2nd ed. Berlin, Germany: Springer-Verlag, 1999, ser. Springer Series on Wave Phenomena.
- [5] T. M. Elfouhaily, S. Guignard, R. Awadallah, and D. R. Thompson, "Local and non-local curvature approximation: A new asymptotic theory for wave scattering," *Waves Random Complex Media*, vol. 13, no. 4, pp. 321–337, Oct. 2003.
- [6] T. M. Elfouhaily and J. T. Johnson, "Extension of the local curvature approximation to third order and full tilt invariance," *Waves Random Complex Media*, vol. 16, no. 2, pp. 97–119, May 2006.
- [7] C. Bourlier and N. Pinel, "Numerical implementation of local unified models for backscattering from random rough sea surfaces," *Waves Random Complex Media*, vol. 19, no. 3, pp. 455–479, Aug. 2009.
- [8] T. Elfouhaily, B. Chapron, K. Katsaros, and D. Vandemark, "A unified directional spectrum for long and short wind-driven waves," *J. Geophys. Res.*, vol. 102, no. C7, pp. 781–796, 1997.
- [9] A. A. Mouche, D. Hauser, J.-F. Daloze, and C. Guérin, "Dual-polarization measurements at C band over the ocean: Results from airborne radar observations and comparison with ENVISAT ASAR data," *IEEE Trans. Geosci. Remote Sens.*, vol. 43, no. 4, pp. 753–769, Apr. 2005.
- [10] C. Bourlier, "Azimuthal harmonic coefficients of the microwave backscattering from a non-Gaussian ocean surface with the first-order SSA model," *IEEE Trans. Geosci. Remote Sens.*, vol. 42, no. 11, pp. 2600–2611, Nov. 2004.
- [11] A. G. Voronovich and V. U. Zavorotny, "Theoretical model for scattering of radar signals in Ku- and C-bands from a rough sea surface with breaking waves," *Waves Random Complex Media*, vol. 11, no. 3, pp. 247–269, Jul. 2001.
- [12] A. A. Mouche, B. Chapron, and N. Reul, "A simplified asymptotic theory for ocean surface electromagnetic wave scattering," *Waves Random Complex Media*, vol. 17, no. 3, pp. 321–341, Aug. 2007.
- [13] I. S. Gradshteyn and I. M. Ryzhik, *Table of Integrals, Series, and Products*. New York: Academic, 2000.